

NASA Technical Memorandum 4328

Preliminary Flight Evaluation of an Engine Performance Optimization Algorithm

H. H. Lambert, G. B. Gilyard,
J. D. Chisholm, and L. J. Kerr

OCTOBER 1991



NASA Technical Memorandum 4328

Preliminary Flight Evaluation of an Engine Performance Optimization Algorithm

H. H. Lambert and G. B. Gilyard
Dryden Flight Research Facility
Edwards, California

J. D. Chisholm
McDonnell Douglas Corporation
McDonnell Aircraft Company
St. Louis, Missouri

L. J. Kerr
Pratt & Whitney
Government Engine and Space Business
West Palm Beach, Florida



National Aeronautics and
Space Administration
Office of Management
Scientific and Technical
Information Program

1991

PRELIMINARY FLIGHT EVALUATION OF AN ENGINE PERFORMANCE OPTIMIZATION ALGORITHM

H.H. Lambert* and G.B. Gilyard**
NASA Dryden Flight Research Facility
Edwards, California

J.D. Chisholm†
McDonnell Aircraft Company
McDonnell Douglas Corporation
St. Louis, Missouri

L.J. Kerr‡
Pratt & Whitney
Government Engine and Space Business
West Palm Beach, Florida

Abstract

The initial flight test evaluation phase of the performance seeking control (PSC) algorithm has been completed for one engine, subsonic, part power, and military power operation on an F-15 aircraft, using a PW1128 engine. The algorithm is designed to optimize the quasi-steady-state performance of an engine for three primary modes of operation: the minimum fuel, the minimum fan turbine inlet temperature (*FTIT*), and the maximum thrust modes. The minimum fuel mode is designed to minimize thrust-specific fuel consumption during cruise conditions. The minimum *FTIT* mode is designed to extend the turbine life by decreasing the *FTIT* during cruise and accelerating flight conditions. The maximum thrust mode is designed to maximize net propulsive force at military power. Decreases in thrust-specific fuel consumption of approximately 1 percent have been measured in the minimum fuel mode; integrated over the life of the aircraft and fleet size, these fuel savings are significant. Decreases of up to approximately 100 °R in *FTIT* were measured in the minimum *FTIT* mode. Temperature reductions of this magnitude are significant and would more than double engine life if *FTIT* were the only factor. Thrust increases of up to approximately 12 percent were measured in the maximum thrust mode. The system dynamics of the closed-loop algorithm operation appear good. The preliminary flight phase has provided a general validation of the

PSC technology which can provide significant benefits to the next generation of fighter and transport aircraft.

Nomenclature

<i>AAHT</i>	high-pressure turbine area component deviation parameter, in ²
<i>AJ</i>	nozzle throat area, in ²
<i>AJNL</i>	effective nozzle throat area, in ²
<i>BLD</i>	bleed air flow, lb/sec
<i>CEM</i>	compact engine model
<i>CIM</i>	compact inlet model
<i>CIVV</i>	compressor inlet variable guide vane, deg
<i>CPSM</i>	compact propulsion system model
<i>DEEC</i>	digital electronic engine control
<i>DEHPT</i>	high-pressure turbine component deviation parameter, percent
<i>DELPT</i>	low-pressure turbine component deviation parameter, percent
<i>DINL</i>	inlet drag, lb
<i>DNOZ</i>	nozzle drag, lb
<i>DRAM</i>	ram drag, lb
<i>DWFAN</i>	fan airflow component deviation parameter, lb/sec
<i>DWHPC</i>	high-pressure compressor airflow component deviation parameter, lb/sec
<i>EMD</i>	engine model derivative
<i>EPR</i>	engine pressure ratio, <i>PT6</i> / <i>PT2</i>
<i>F</i>	steady-state variable model sensitivity matrix

*Aerospace Engineer. Member AIAA.

**Aerospace Engineer.

†Propulsion Engineer. Member ASME.

‡Systems Engineer.

Copyright ©1991 by the American Institute of Aeronautics and Astronautics, Inc. No copyright is asserted in the United States under Title 17, U.S. Code. The U.S. Government has a royalty-free license to exercise all rights under the copyright claimed herein for Governmental purposes. All other rights are reserved by the copyright owner.

<i>FG</i>	gross thrust, lb
<i>FN</i>	net thrust, lb
<i>FNP</i>	net propulsive force, lb
<i>FTIT</i>	fan turbine inlet temperature, °R
HIDEC	highly integrated digital electronic control
<i>HPX</i>	power extraction, hp
<i>h</i>	altitude
<i>M</i>	Mach number
MIL	military
<i>N1</i>	fan rotor speed, rpm
<i>N1C2</i>	fan rotor speed, corrected to station 2, rpm
<i>N2</i>	compressor rotor speed, rpm
<i>P_{amb}</i>	ambient pressure, lb/in ²
<i>PB</i>	burner pressure, lb/in ²
PCM	pulse code modulation
PLA	power lever angle, deg
<i>PS</i>	static pressure, lb/in ²
PSC	performance seeking control
PSM	propulsion system matrix
<i>PT</i>	total pressure, lb/in ²
<i>RCVV</i>	rear compressor variable guide vanes, deg
<i>SMF</i>	fan stall margin
<i>SMHC</i>	high-pressure compressor stall margin
SSIM	steady-state inlet model
SSVM	steady-state variable model
SVM	state variable model
TLER	turbine life exhaustion rate, life/hr
<i>TMT</i>	composite metal temperature, °R
<i>TSFC</i>	thrust-specific fuel consumption, sec ⁻¹
<i>TT</i>	total temperature, °R
<i>WCFAN</i>	fan airflow, lb/sec
<i>WCHPC</i>	high-pressure compressor airflow, lb/sec
<i>WF</i>	gas generator fuel flow, lb/hr
<i>u</i>	vector of control variables in the SVM
<i>u_i</i>	vector of control variables in the CIM
<i>u_m</i>	vector of control variables in the SSVM
<i>u_p</i>	vector of control variables in the linear programming problem
<i>x</i>	vector of state variables in the SVM
<i>y</i>	vector of output variables in the SSVM
<i>y_i</i>	vector of output variables in the CIM
<i>y_m</i>	vector of output variables in the SVM

y_p vector of output variables in the linear programming problem

Prefix

Δ perturbation

∂ partial

Suffix, PW1128 engine station numbers, ref. Fig. 3

2 fan inlet

2.5 compressor inlet

3 compressor discharge

4 high-pressure turbine inlet

6 afterburner discharge inlet

7 nozzle throat discharge

Superscript

T transpose

Introduction

The increasing use of digital engine control has opened up the possibility of significantly improving the performance of aircraft turbofan engines. Control laws for current generation engines are based on classical control theory and empirically developed schedules that must accommodate a wide range of engine health and off-nominal operation. These schedules are compromised to account for variations in manufacturing tolerances, the uncertainty associated with engine deterioration, and other off-nominal behavior of gas turbine components for a specific engine. Performance improvements can be achieved using sophisticated control algorithms designed to recover the full performance potential of the propulsion system.

The NASA Dryden Flight Research Facility has developed, flight tested, and evaluated propulsion system improvements on the F-15 airplane for over a decade. The F-15 flight research program included the first flight implementation of a full authority digital electronic engine control (DEEC),^{1,2} followed by flight test of an F100 engine model derivative (EMD),³ and most recently implemented a highly integrated digital electronic control (HIDEC) on the engine.^{4,5} The F100 EMD program demonstrated the performance benefits resulting from improved fan, turbine, and afterburner design. The HIDEC program demonstrated performance improvements such as increased thrust and extended turbine life for a nominal engine. Favorable results from the HIDEC study supported further research into adaptive optimization algorithms.

There is considerable interest in developing real-time performance optimization technology for application to high-speed commercial transport and advanced fighter designs. The Air Force has funded an independent performance seeking control study.⁶ The performance benefits demonstrated on the F-15 HIDEC research vehicle, coupled with the Air

Force performance seeking control study, prompted the performance seeking control (PSC) program, currently under flight test evaluation at the NASA Dryden Flight Research Facility. The objective of PSC is to adaptively optimize the near-steady-state performance of an aircraft-propulsion system in real time.

The PSC algorithm has three primary modes of operation: the minimum fuel, the minimum fan turbine inlet temperature (*FTIT*), and the maximum thrust modes. The minimum fuel mode is designed for cruise conditions, the minimum *FTIT* mode is designed for both cruise and accelerating flight conditions, and the maximum thrust mode is primarily intended for use during accelerating flight conditions. The minimum fuel mode minimizes fuel flow while maintaining constant net propulsive force (*FNP*) throughout the maneuver, or effectively minimizes thrust-specific fuel consumption (*TSFC*). During cruise conditions, the minimum *FTIT* mode lowers the *FTIT* while maintaining constant *FNP* throughout the maneuver. During accelerating flight conditions, the minimum *FTIT* mode lowers the *FTIT* while allowing *FNP* to increase with flight condition. The maximum thrust mode maximizes *FNP* at military (MIL) power settings.

The PSC algorithm optimizes the propulsion performance during quasi-steady-state maneuvers by applying trims to the propulsion system. The trim values are determined from an onboard, real-time optimization process. The PSC control law includes an estimation process, a modeling process, and an optimization process. The estimation process uses a Kalman filter to estimate component deviation parameters from flight measurements. The component deviation parameters account for changing levels of engine health, engine-to-engine manufacturing differences, and off-nominal behavior of a specific engine. The modeling process uses linear and nonlinear models to estimate unmeasured engine parameters from flight measurements and the component deviation parameter estimates. The optimization process uses linear programming techniques to determine the optimal engine operating condition for the mode selected. The PSC algorithm relies heavily on accurate models of the inlet and engine system and estimates of unmeasured parameters. Before implementation, the algorithm was tested extensively with simulated data. The parameter estimation and modeling processes have undergone preliminary evaluation using flight test data.⁷ Results indicate the PSC estimation algorithm provides reasonable estimates of the variables needed to optimize the engine operation.

Preliminary flight testing of the various PSC modes was conducted using one of the two F-15 engines. This paper presents qualitative results for the PSC modes at the PSC model design condition and other selected conditions. Flight testing has been restricted to the subsonic flight envelope and for throttle settings up to MIL power. Results

for the steady-state and dynamic behavior of the control law and the performance benefits are discussed.

Airplane and Engine Description

The PSC program has been implemented on the NASA F-15 research airplane (Fig. 1), which is a modified high-performance aircraft capable of speeds in excess of Mach 2.0. The F-15 aircraft is powered by two PW1128 afterburning turbofan engines. The aircraft has been modified with a digital electronic flight control system. Additional information on the F-15 aircraft is found in Ref. 3.

The PW1128 engine is a moderate-bypass ratio, twin-spool, afterburning turbofan technology demonstrator, derived from the F100-PW-100 engine. The engine is controlled by a full-authority DEEC that is similar to the current production F100 engine controller. The DEEC provides both open-loop scheduling and closed-loop feedback control of corrected fan speed (*N1C2*) by way of the fuel flow (*WF*) and engine pressure ratio (*EPR*) by way of the nozzle throat area (*AJ*). The compressor inlet variable guide vane (*CIVV*) and rear compressor variable vane (*RCVV*) positions are scheduled on rotor speeds by way of open-loop control. The DEEC software has been modified to accommodate PSC; however, the normal DEEC control loops (that is, *N1C2* and *EPR*) have not been modified. A more detailed description of the PW1128 engine is in Ref. 2.

A diagram of the PW1128 engine is shown in Fig. 2. The locations of the DEEC instrumentation, the DEEC calculated parameters, and the parameters estimated by PSC are indicated. Fan airflow (*WCFAN*) and engine face total pressure (*PT2*) are independently modeled by both the DEEC and PSC control laws. The PSC algorithm requires only conventional DEEC instrumented parameters as inputs and estimates other necessary parameters within the algorithm. The engine instrumentation and a wide range of internal PSC algorithm parameters are sampled at 20 Hz. The airdata are obtained from the F-15 production side probes. The algorithm corrects the data for position error and location effects. The airdata are recorded at 20 Hz. All data are recorded on a pulse code modulation (PCM) system.

Performance Seeking Control Law Algorithm

The general structure of the PSC algorithm involves calculating optimal control trim commands for a propulsion system model that is continuously updated. A flow diagram of the algorithm is given in Fig. 3. The control law has estimation, modeling, and optimization processes. The estimation process is a Kalman filter estimation of five component deviation parameters designed to account for the off-nominal behavior of the engine during flight. The second step formulates and uses the compact propulsion system model (CPSM) to estimate unmeasured engine outputs,

such as component stall margins, required for an optimal solution.

Flight measurements are used to look up model data and as direct inputs to both the Kalman filter and the CPSM. The component deviation parameter estimates are also input to the CPSM. The estimates cause the CPSM outputs to more accurately reflect the actual engine operating condition. A propulsion system matrix (PSM) derived from the CPSM is the basis of the optimization process. Because of the non-linearity of the problem, each set of optimal trims does not necessarily represent the final solution. The final solution must be converged to over time. Additional information on the structure and design of the PSC algorithm is available in Ref. 8. The PSC algorithm is an outer-loop controller and does not effect the normal engine DEEC control loops *N1C2* and *EPR*.

Kalman Filter

The first step in the PSC algorithm is to identify the off-nominal characteristics of the engine when operating at or near steady-state conditions. This is done by estimating five component deviation parameters with a Kalman filter: the low- and high-pressure turbine efficiency component deviation parameters (*DELPT* and *DEHPT*), the fan and high-pressure compressor airflow component deviation parameters (*DWFAN* and *DWHPC*), and the high-pressure turbine area component deviation parameter (*AAHT*). The *DELPT* and *DEHPT* are related to the changes from nominal in the low- and high-pressure turbine efficiency. The *DWFAN* and *DWHPC* are related to the changes from nominal in fan and high-pressure compressor airflow. The *AAHT* is related to changes from nominal in the high-pressure turbine area. These parameters are used to adjust the nominal CPSM to match the actual engine operating condition. The state variable model (SVM) is used in the design and implementation of the Kalman estimator. The SVM is a piecewise linear model covering the entire range of engine operation at Mach 0.90 at an altitude of 30,000 ft, at standard day conditions. The estimator consists of a state-space perturbation model, an associated table of steady-state trim values for all the engine variables in the model, and some extended nonlinear calculations. The SVM model data are a function of *PT4* and *PT6*. The state, control, and measurement vectors are defined as

$$x = [N1 \ N2 \ TMT \ DEHPT \ DELPT \ DWFAN \ DWHPC \ AAHT]^T$$

$$u = [WF \ AJ \ CIVV \ RCVV \ HPX \ BLD]^T$$

$$y = [PT6 \ PT4 \ FTIT \ N1 \ N2]^T$$

The locations of the engine parameters are shown in Fig. 2. Values for the following measurements and control variables are taken directly from flight data: *N1*, *N2*, *PB*, *FTIT*, *PT6*, *WF*, *AJ*, *CIVV*, and *RCVV*. The *PT4* is modelled as a function of *PB*, *HPX* is modelled as a func-

tion of *N2*, and *BLD* is modelled as a function of Mach and altitude. Additional engine and flight parameters are used indirectly by the Kalman filter to calculate other engine variables and to transform the engine data to the SVM design condition of Mach 0.90 at an altitude of 30,000 ft. Multipliers that are functions of *PT2* and *TT2* are used to transform the measured and calculated engine variables to different flight conditions. Additional information on the Kalman filter is found in Refs. 8 and 9.

Compact Propulsion System Model

The second step in the PSC algorithm is formulation of the CPSM. The CPSM combines two smaller compact models, the compact engine model (CEM) and the compact inlet model (CIM), that together model the propulsion system and form the basis for the optimization process.

Compact Engine Model

The CEM consists of a linear steady-state perturbation model, referred to as the steady-state variable model (SSVM), and follow-on nonlinear calculations, including nozzle effects. The SSVM is of the form

$$y_m = F u_m$$

It has a design condition of Mach 0.90 at an altitude of 30,000 ft, but has been transformed to a sea level static reference condition for implementation. The u_m and y_m variables represent the SSVM control input and measurement vectors, respectively. They are defined as

$$u_m = [WF \ PT6 \ CIVV \ RCVV \ HPX \ BLD \ DEHPT \ DELPT \ DWFAN \ DWHPC \ AAHT]^T$$

$$y_m = [N1 \ N2 \ PT2.5 \ PT4 \ TT2.5 \ TT3 \ TT4 \ FTIT \ TT6 \ WCFAN \ WCHPC]^T$$

The SSVM uses engine measurements for the following control inputs: *WF*, *PT6*, *CIVV*, and *RCVV*. The *HPX* and *BLD* are modelled as in the Kalman filter. The locations of the engine parameters are shown in Fig. 2. The Kalman filter estimates of the component deviation parameters are input to the SSVM calculation as part of the control vector. The control inputs are transformed to the SSVM sea level static reference condition using multipliers that are a function of *PT2* and *TT2*. The SSVM provides estimates of the following variables at sea level static conditions: *N1*, *N2*, *AJ*, *PT2.5*, *PT4*, *TT2.5*, *TT3*, *TT4*, *FTIT*, *TT6*, *WCFAN*, and *WCHPC*. These estimates are then transformed to the original flight condition for use in the subsequent nonlinear CEM calculations. Several of the variables estimated by the SSVM are also instrumented: *N1*, *N2*, *AJ*, and *FTIT*.

Following completion of the linear SSVM calculation, the nonlinear CEM estimates are calculated at the original

flight condition. These variables include *PT7*, *TT7*, *FG*, *FN*, *DRAM*, *DNOZ*, *AJNL*, *SMF*, and *SMHC*. The nonlinear calculations use a combination of analytical equations and empirically derived data tables. They are based on both measured engine variables and SSVM estimates. If a variable is both measured and estimated, the flight measurement is used in the nonlinear calculations. The nonlinear calculations for *SMF*, *SMHC*, *AJNL*, and *FN* are linearized with respect to *WF*, *PT6*, *CIVV*, and *RCVV* in real time. The partials produced are used in the follow-on optimization process. Additional information on the CEM calculations is available in Refs. 7 and 8.

Compact Inlet Model

The subsonic CIM consists of a nonlinear calculation of inlet drag (*DINL*) and the inlet *PT2*. At subsonic flight conditions, the nominal inlet schedules are optimal, and inlet geometry is not included in the PSC algorithm at subsonic conditions. Both *DINL* and the inlet *PT2* are calculated as a function of Mach, *WCFAN*, and P_{amb} . The PSC algorithm linearizes the *PT2* and *DINL* calculations with respect to *WCFAN* in real time. The result is a linear steady-state perturbation model of the inlet. The u_i and y_i represent the control input and measurement vectors, respectively. At subsonic conditions, they are defined as

$$u_i = [WCFAN]$$

$$y_i = [PT2 \text{ } DINL]^T$$

Additional information on the CIM is available in Ref. 8.

Optimization Process

The subsonic phase of the PSC program optimizes the combined performance of the inlet and engine. The PSC algorithm uses linear programming techniques to determine the optimal engine control states. The linear programming optimization is based on a linear steady-state model referred to as the PSM. Linear models from the CEM and CIM are integrated to form the PSM. The PSM control and output vectors u_p and y_p are defined as

$$u_p = [WF \text{ } PT6 \text{ } CIVV \text{ } RCVV]^T$$

$$y_p = [N1C2 \text{ } N2 \text{ } WCFAN \text{ } TT3 \text{ } FTIT \text{ } SMF \text{ } SMHC \text{ } AJ \text{ } FNP]^T$$

The engine parameters are shown in Fig. 2.

The linear programming problem determines the optimum subject to a specific set of constraints. Each control and output variable has associated constraints that are used in the formulation of the linear programming problem. The constraints are functions of engine hardware, empirical data, and the desired goal of the optimization. The local opti-

mal engine operating point is determined by iterating on the CPSM modeling-optimization process a specified number of times. The iterative process is referred to as inner looping. The component deviation parameters are assumed constant during the inner looping. Once the inner looping is completed, the engine interface logic determines the trims required to achieve the current optimal operating conditions. The current PSC configuration uses 12 iterations to determine each set of optimal trims. This iterative process takes approximately 5 sec.

DEEC Interface and Supervisory Logic

In addition to the PSC control law, the PSC system includes logic to interface with the DEEC, as well as logic to monitor and assure safe engine operation. The DEEC interface logic calculates the DEEC trims required to achieve the PSC optimal engine operating condition. Supervisory logic was developed to oversee the PSC operation. The engine operation is monitored to protect against fan stalls, and trims are modified if necessary. Supervisory logic also monitors the engine for transients resulting from PLA changes. The PSC algorithm is designed for quasi-steady-state engine operation. Therefore, PSC is suspended during engine transients and the engine reverts to baseline operation. The DEEC applies the PSC trims to the engine, subject to standard DEEC protection. The DEEC does not permit limits to be exceeded and, as such, overrides the PSC trims as necessary.

Flight Test Results

The three PSC modes have undergone preliminary subsonic flight testing. Maneuvers were flown on the F-15 aircraft to evaluate the performance benefits and the dynamic behavior of each mode. The engine data given in this paper were obtained from the following sources: the *WF*, *AJ*, *CIVV*, *RCVV*, and *PT6* were recorded from the right-hand test engine; the engine pressure ratio (*EPR*) and *WCFAN* data were recorded from the DEEC; the *FNP* was recorded from the PSC algorithm; and the *TSFC* was calculated postflight.

Minimum Fuel Mode

The minimum fuel mode is designed to minimize fuel flow (effectively *TSFC*) while maintaining constant *FNP* during cruise conditions. The maneuvers flown consisted of flying at stabilized flight conditions with the PSC system engaged. The aircraft was allowed to stabilize at the cruise conditions before PSC was engaged. Data were recorded for approximately 2 min with PSC engaged. After 2 min, the PSC system was disengaged, and another 2 min of data representing the baseline engine were recorded. The maneuvers were flown back-to-back to allow for direct comparisons by minimizing the effects of variations in the test day conditions.

The minimum fuel mode was evaluated at two conditions: Mach 0.90 at an altitude of 30,000 ft and a power level angle (PLA) of 40°, and Mach 0.88 at an altitude of 45,000 ft and a PLA of 40°. The first condition represents the PSC model design point. The baseline performance schedules are efficient at Mach 0.90 at an altitude of 30,000 ft and a PLA of 40°. Thus, small benefits were expected. It is, however, the point in the flight envelope where the estimation processes are expected to be the most accurate, as the linear models were derived at this condition. The second cruise condition of Mach 0.88 at an altitude of 45,000 ft was selected to evaluate the mode operation at off-design conditions. This flight condition is near the maximum range cruise condition for the aircraft. To maintain constant flight conditions and constant test engine PLA during the maneuvers, the left throttle was modulated manually by the pilot to maintain Mach number.

Figure 4 shows the results for the cruise point of Mach 0.90 at an altitude of 30,000 ft. Time histories are given for the engine and linear programming control variables (WF , AJ , $CIVV$, $RCVV$, and $PT6$), the algorithm performance variables (WF , FNP , and $TSFC$), and engine pressure ratio (EPR) and $WCFAN$. The EPR is defined as $PT6/PT2$. The PSC algorithm was engaged from 10 to 130 sec, as shown on the time histories. Dynamics caused by engaging PSC are apparent in both WF and FNP until approximately 75 sec. Thus, steady-state results pertain to the 75- to 130-sec part of the maneuver. The steady-state value of $TSFC$ with PSC engaged was approximately 1.17. The PSC algorithm held FNP to within ± 2 percent of the initial value. Turning PSC off caused both WF and FNP to decrease in the steady state. The steady-state $TSFC$ for the nominal engine was 1.18, slightly greater than with PSC on. The modest decrease in $TSFC$ was expected at this flight condition, as the baseline controller is efficient at Mach 0.90 at an altitude of 30,000 ft and a PLA of 40°.

In general, the dynamic behavior of the engine was good (Fig. 4). Transient dynamics are observed until 75 sec after PSC was engaged and are partially an artifact of the steady-state assumptions of the algorithm design. The WF , $PT6$, and AJ showed slight variations during the remainder of the maneuver with PSC on, but the variations were not significant. The small decrease in $TSFC$ was achieved by decreasing WF to the engine, while trimming $CIVV$, $RCVV$, and AJ to maintain thrust. The key variables in the minimum fuel linear programming problem are WF and $PT6$. The $PT6$ is effected by AJ . Decreasing WF will decrease FNP , assuming all other variables are constant. Increasing AJ decreases EPR and increases $WCFAN$, assuming all other variables are constant. At lower fan airflows, $WCFAN$ is more sensitive to the perturbation in AJ than at higher airflows. The FNP is affected by EPR and $WCFAN$, and the relative sensitivities of FNP to these parameters varies with engine operating condition. Decreasing either EPR or $WCFAN$ while holding the other param-

eter constant decreases FNP . In the minimum fuel mode, the PSC algorithm decreases WF and uses $PT6$ to balance EPR and $WCFAN$ to hold the desired FNP . With the linear programming problem, the limiting constraints are

$$FNP = \text{constant}$$

$$\Delta FNP = (\partial FNP / \partial u_p) \Delta u_p$$

For this particular test maneuver, PSC trims AJ to increase $WCFAN$ and decrease EPR to maintain FNP (Fig. 4). The $CIVV$ and $RCVV$ trims contribute to the $WCFAN$ increase, but their effect is small compared to that of AJ . The small differences in the WF , EPR , and $WCFAN$ (Fig. 4) between PSC on and off indicate that the baseline schedules are efficient for this condition.

The results for the cruise maneuver at Mach 0.88 at an altitude of 45,000 ft and a PLA of 40° are shown in Fig. 5. Time histories are given for the engine and linear programming control variables (WF , AJ , $CIVV$, $RCVV$, and $PT6$), and algorithm performance variables (WF , FNP , and $TSFC$), and EPR and $WCFAN$. The PSC algorithm was engaged from 20 to 140 sec, as shown on the time histories.

The algorithm appeared to settle more quickly than at Mach 0.90 at an altitude of 30,000 ft, and the dynamics induced by engaging PSC are less pronounced. The engine response is slower at this condition than at Mach 0.90 at an altitude of 30,000 ft, and PSC is better able to track the engine dynamics. The PSC algorithm held FNP to within ± 2 percent of the initial value. The steady-state value of $TSFC$ with PSC engaged is approximately 1.04 at 125 sec. Between 125 and 140 sec, FNP is decreasing, causing the noticeable increase in $TSFC$ (Fig. 5). The mean value for the $TSFC$ for the baseline engine is approximately 1.06, greater than with PSC on. The decrease in $TSFC$ at this condition was achieved by the same mechanism described for the Mach 0.90 maneuver at 30,000 ft. Again, PSC decreases the WF while trimming AJ to balance EPR and $WCFAN$ to maintain FNP . For this maneuver, AJ was trimmed to increase $WCFAN$ and decrease EPR (Fig. 5).

The baseline performance schedules are less efficient at Mach 0.88 at an altitude of 45,000 ft than at Mach 0.90 at an altitude of 30,000 ft. Thus, the steady-state differences with PSC on and off are more pronounced (Fig. 5). The relationship between the optimal and baseline engine operating conditions is a function of the baseline performance schedules, and would be different if the baseline schedules were defined differently.

The minimum fuel mode has performed as expected at most flight-throttle settings. The decreases in $TSFC$ of 1 to 2 percent translate to significant fuel savings when integrated over the life of the aircraft and fleet. At some throttle settings, though, PSC appears to increase rather than decrease $TSFC$. The problem is currently under investigation.

Minimum *FTIT* Mode

The minimum *FTIT* mode is designed to decrease the *FTIT* while maintaining *FNP* levels during both cruise and accelerating flight conditions. Engine turbine life can be expressed as turbine life exhaustion rate (TLER). Figure 6 shows TLER as a function of turbine temperature relative to the turbine melting temperature. The temperature ranges given represent typical engine operating temperatures. Overall turbine life is determined by the cumulative impact of TLER at different operating conditions over the aircraft mission. Lowering the *FTIT* decreases the TLER, resulting in extended turbine-combustor life.

The minimum *FTIT* mode was evaluated at Mach 0.90 at an altitude of 25,000 ft, MIL power, and over the Mach range of 0.75 to 0.95 at an altitude of 45,000 ft, MIL power. The maneuvers flown were similar to the maneuvers used to evaluate the minimum fuel mode. The aircraft was allowed to stabilize at the cruise condition with PSC off. The PSC algorithm was then engaged, and data were recorded for approximately 2 min. The PSC was turned off, and data representing the baseline engine were recorded for another 2 min. The maneuvers were flown back-to-back to minimize the effects of variations in the test day conditions.

Figure 7 shows the results for the Mach 0.85 cruise point at an altitude of 45,000 ft. Time histories are given for the engine and linear programming control variables (*WF*, *AJ*, *CIVV*, *RCVV*, and *PT6*), and the algorithm performance variables (*FNP* and *FTIT*), and *EPR* and *WCFAN*. The PSC was engaged from 10 to 125 sec, as shown on the time histories. The steady-state value of *FTIT* with PSC engaged was 2050 °R. The PSC algorithm increased *FNP* by 5 percent over the initial *FNP*, although the variation in *FNP* with PSC engaged was within ± 1 percent. The steady-state value of *FTIT* for the baseline engine was 2150 °R. The PSC algorithm decreased the *FTIT* by 100 °R, and increased *FNP* slightly (Fig. 7). The *FTIT* decrease may have been greater if the algorithm had held the initial *FNP* value more closely.

With PSC engaged, *WF*, *CIVV*, and *RCVV* were well behaved dynamically, while *AJ* exhibited a small amplitude oscillation of ± 5 in² (Fig. 7). The decrease in *FTIT* was achieved by trimming *WF*, *AJ*, *CIVV*, and *RCVV* to decrease *WCFAN* and thus the *FTIT*, while increasing the *EPR* to maintain *FNP*. The algorithm decreased *AJ* to balance the *WCFAN* and *EPR* to maintain constant *FNP*.

Figure 8 shows predicted and flight-measured decreases in *FTIT* for various test points as a function of Mach and altitude. In all the cases, the throttle was at MIL power. In general, PSC performed as predicted in the minimum *FTIT* mode. Decreases of up to 100 °R were measured at an altitude of 45,000 ft. Decreases of 20 °R were mea-

sured at Mach 0.90 at an altitude of 25,000 ft. Temperature reductions of this magnitude are significant and, as shown in Fig. 6, would double engine life if *FTIT* were the only factor. The goals for this mode were achieved as PSC obtained *FTIT* reductions while *FNP* was held constant.

Maximum Thrust Mode

The maximum thrust mode is designed to maximize *FNP* at MIL power. The maneuver flown consisted of stabilizing the engines at MIL power in a windup turn at Mach 0.50. The aircraft was then rolled to wings level and allowed to accelerate to Mach 0.95 at a constant altitude of 30,000 ft. The maneuver was executed twice, once with PSC off and once with PSC on. The accelerations were flown back-to-back to minimize the effects of variation in test day conditions.

Figure 9 shows time history comparisons of several engine variables for back-to-back maneuvers with PSC on and PSC off. Engine and linear programming control variables (*WF*, *AJ*, *CIVV*, *RCVV*, and *PT6*), the performance variable (*FNP*), and *EPR* and *WCFAN* are given as a function of Mach number. The PSC algorithm increased *FNP* by 10 to 12 percent above the nominal thrust level, resulting in a substantial increase in acceleration. The PW1128 engine has conservative schedules because it was a technology demonstrator. The schedules would be more efficient in a production engine, and the engine manufacturer estimates that thrust increases of approximately 4 to 6 percent would be accrued with a production engine. The algorithm increased the *FNP* by increasing the *WF* and *EPR* (Fig. 9). The *CIVV*, *RCVV*, and *WCFAN* with PSC engaged were close to the nominal values, and *CIVV* and *WCFAN* were at physically limited values. The PSC algorithm decreased *AJ* and increased *EPR* and *WF* to maintain the maximum *WCFAN* (Fig. 9).

The optimal solution to the linear programming problem was bounded by different pairs of constraints as the maneuver progressed. Active linear programming problem constraints for the maneuver with PSC engaged are shown as a function of Mach number in Fig. 10. Active constraints included absolute minimum *AJ* and *SMHC* constraints, absolute maximum *N1* and *FTIT* constraints, and a constraint on the maximum corrected *PT6*. The *AJ* constraint is an actual engine hardware constraint. The *FTIT* and *N1* constraints are obtained from the DEEC control laws. The *SMHC* constraint was empirically derived from ground test data and simulation runs. Predominant constraints for this maneuver are the maximum *N1* and *FTIT*, and the minimum *AJ* limits.

Dynamically, the mode is stable with no oscillations present in the engine response parameters or control effectors. In general, the maximum thrust mode has performed well, demonstrating significant thrust increases at MIL power.

Concluding Remarks

The initial flight test evaluation phase of the performance seeking control (PSC) algorithm has been completed for one engine, subsonic, part power, and military power operation on an F-15 aircraft. A qualitative evaluation of the three major modes of operation indicate that the algorithm is, in general, performing as designed. Thrust increases of up to 12 percent in the maximum thrust mode resulted in substantial increases in acceleration. Decreases of up to approximately 100 °R in fan turbine inlet temperature (FTIT) were measured in the minimum FTIT mode. Temperature reductions of this magnitude are significant and would more than double engine life if FTIT were the only factor. Decreases of thrust-specific fuel consumption (TSFC) of approximately 1 percent have also been measured in the minimum fuel mode; integrated over the life of the aircraft and fleet size, these fuel savings are significant. Problems such as low-amplitude oscillations in the minimum FTIT mode and some TSFC discrepancies in the minimum fuel mode at selected throttle settings were noted. However, these problems are not major and are being resolved. The system dynamics of the closed-loop algorithm operation appear good.

This preliminary flight phase has provided a general validation of the PSC technology objectives. The PSC technology can provide significant benefits to the next generation of fighter and transport aircraft.

References

¹ Burcham, F.W., Jr., Myers, L.P., and Walsh, K.R., *Flight Evaluation of a Digital Electronic Engine Control in a F-15 Airplane*, NASA TM-84918, 1983.

² *Digital Electronic Engine Control (DEEC) Flight Evaluation in an F-15 Airplane*. Proceedings of a mini-

symposium held at the NASA Dryden Flight Research Facility, Edwards, California, May 25-26, 1983, NASA CP-2298.

³ Myers, Lawrence P., and Burcham, Frank W., Jr., *Preliminary Flight Test Results of the F100 EMD Engine in an F-15 Airplane*, NASA TM-85902, 1984.

⁴ Baer-Riedhart, Jennifer L., and Landy, Robert J., *Highly Integrated Digital Electronic Control—Digital Flight Control, Aircraft Model Identification and Adaptive Engine Control*, NASA TM-86793, 1987.

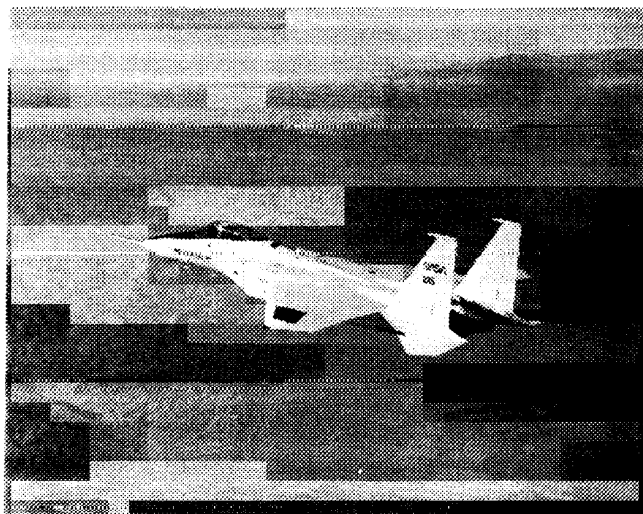
⁵ *Highly Integrated Digital Electronic Control Symposium*. Proceedings of a conference held at the NASA Dryden Flight Research Facility, Edwards, California, March 11-12, 1987, NASA CP-3024.

⁶ Tich, Eric J., Shaw, Peter D., Berg, Donald F., Adibhatla, Shrider, Swan, Jerry A., and Skira, Charles A., "Performance Seeking Control for Cruise Optimization in Fighter Aircraft," AIAA-87-1929, June 1987.

⁷ Maine, Trindel A., Gilyard, Glenn B., and Lambert, Heather H., *A Preliminary Evaluation of an F100 Engine Parameter Estimation Process Using Flight Data*, NASA TM-4216, 1990.

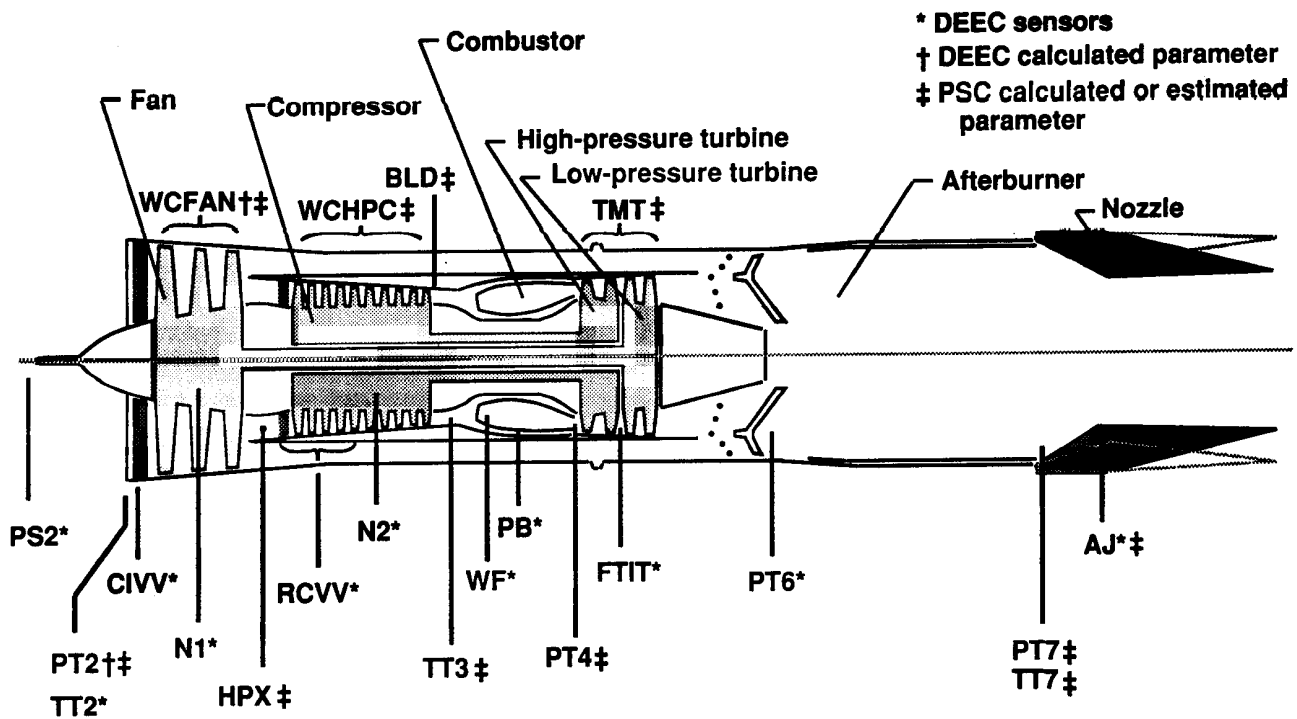
⁸ Smith, R.H., Chisholm, J.D., and Stewart, J.F., "Optimizing Aircraft Performance with Adaptive, Integrated Flight/Propulsion Control," ASME-90-GT-252, presented at the Gas, Turbine and Aeroengine Congress and Exposition, Brussels, Belgium, June 1990.

⁹ Luppold, R.H., Roman, J.R., Gallops, G.W., and Kerr, L.J., "Estimating In-Flight Engine Performance Variations Using Kalman Filter Concepts," AIAA-89-2584, July 1989.



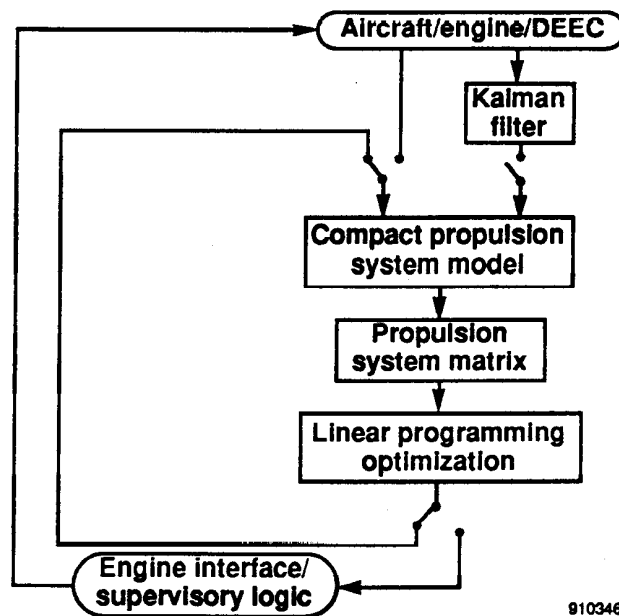
EC 90 312-11

Fig. 1. The F-15 aircraft.



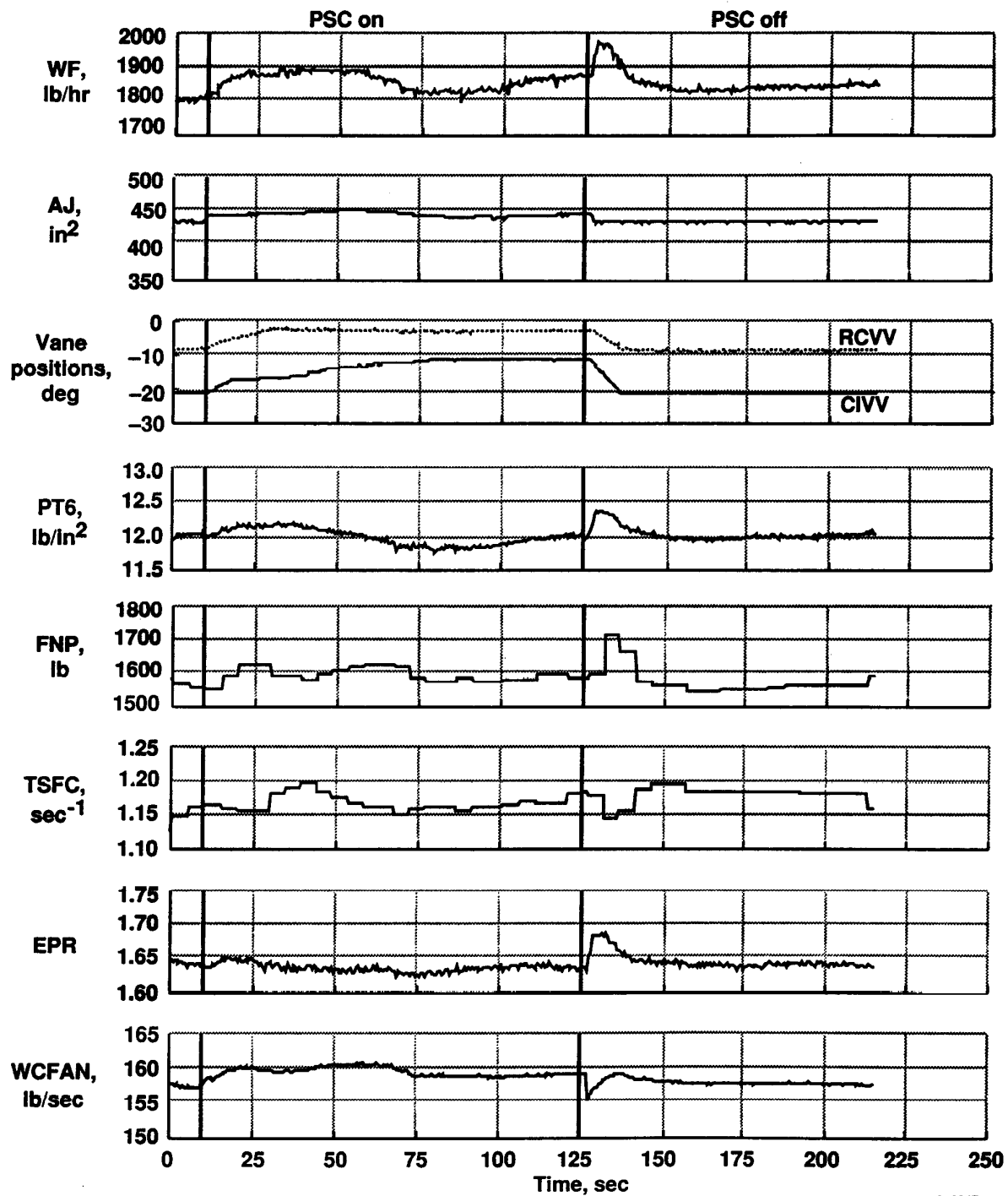
900179

Fig. 2. PW1128 engine sensor and parameter locations.



910346

Fig. 3. Performance seeking control flow diagram.



910347

Fig. 4. Engine parameter time histories for minimum fuel mode evaluation; $M = 0.90$, $h = 30,000$ ft, $PLA = 40^\circ$.

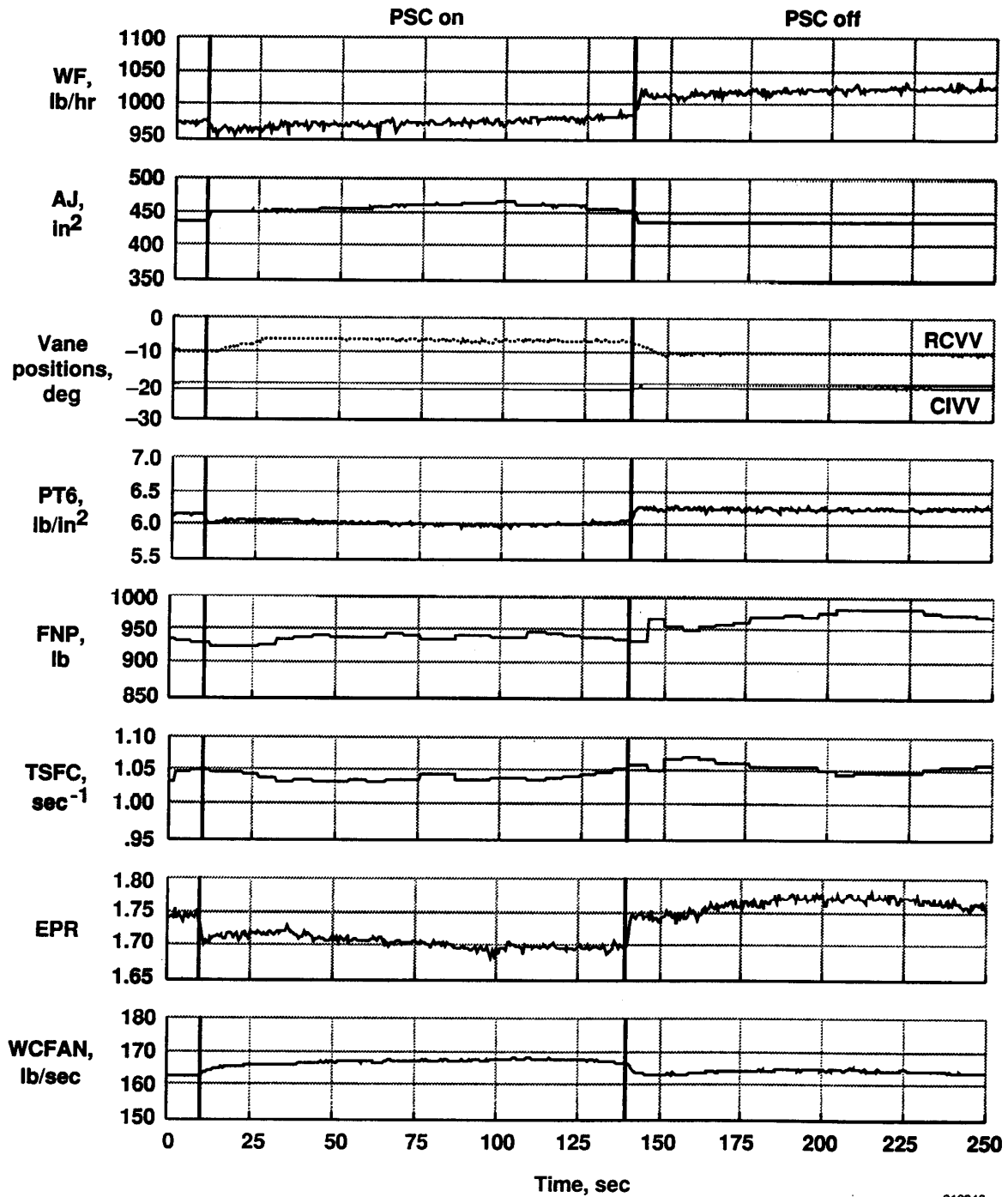
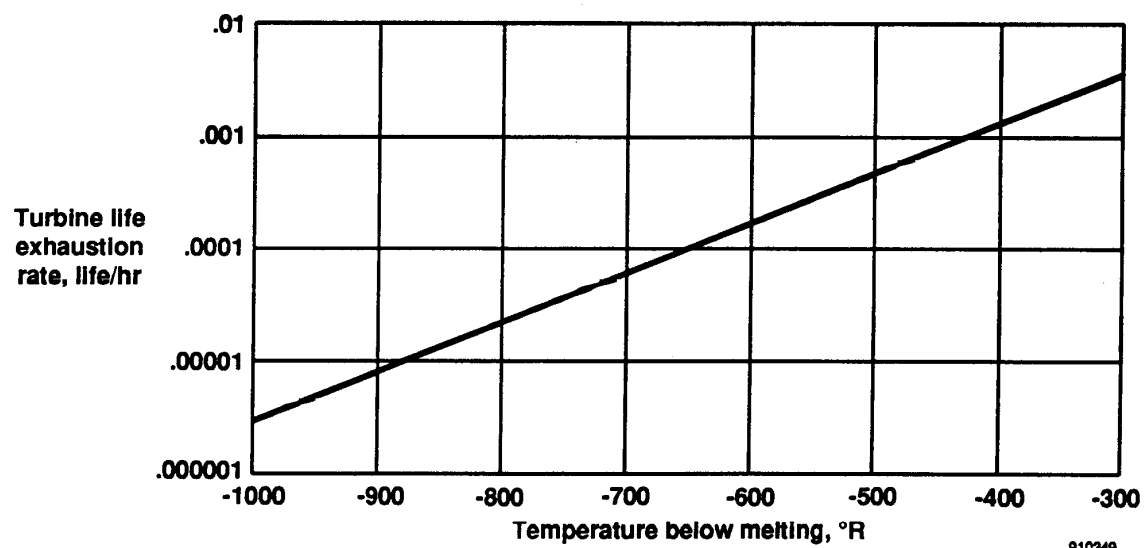
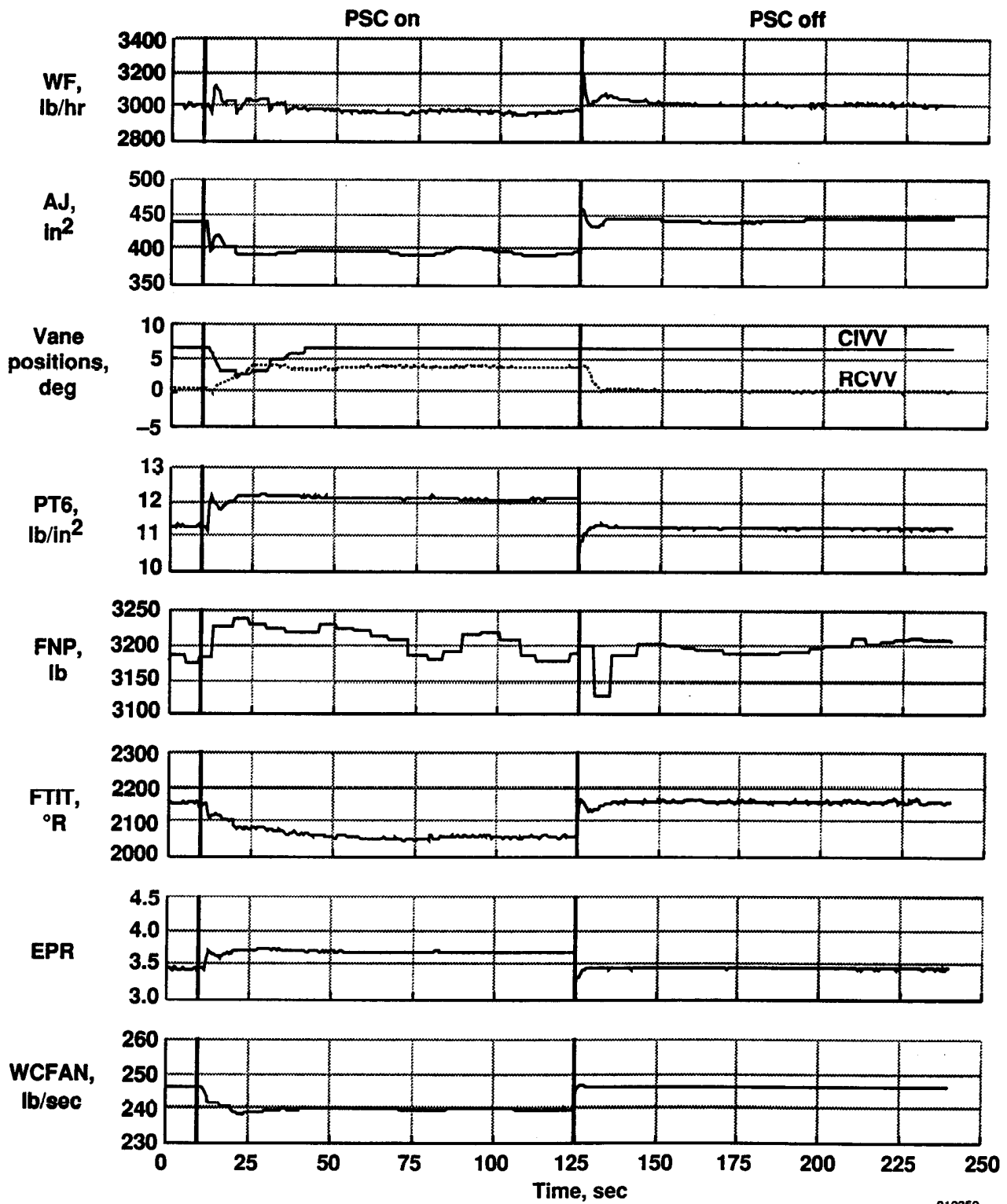


Fig. 5. Engine parameter time histories for minimum fuel mode evaluation; $M = 0.88$, $h = 45,000$ ft, $PLA = 40^\circ$.



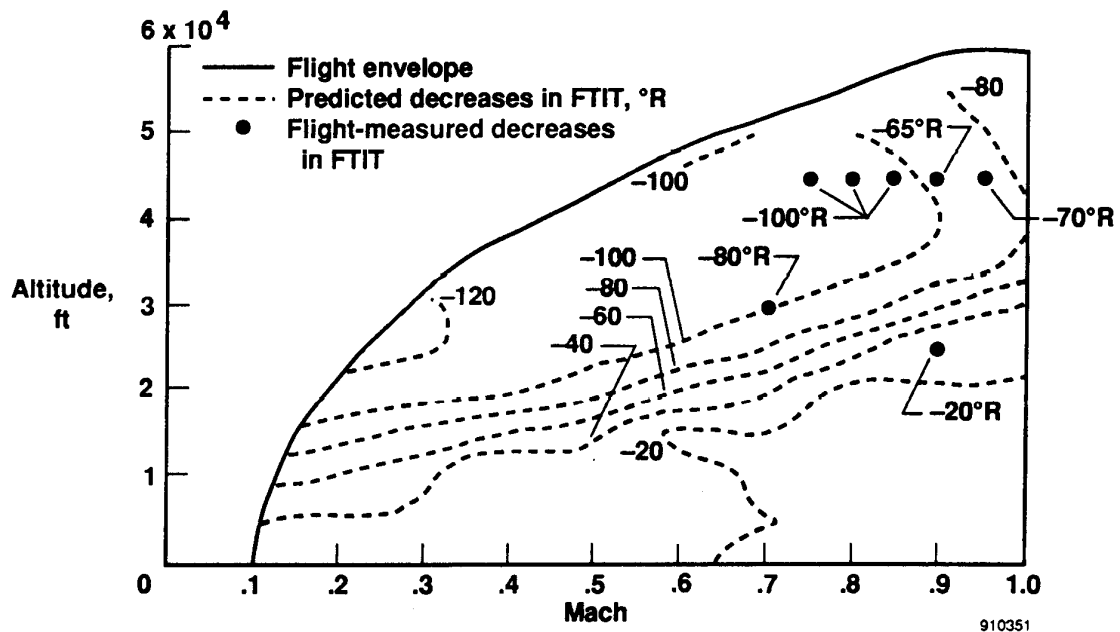
910349

Fig. 6. Turbine life exhaustion rate as a function of turbine temperature.



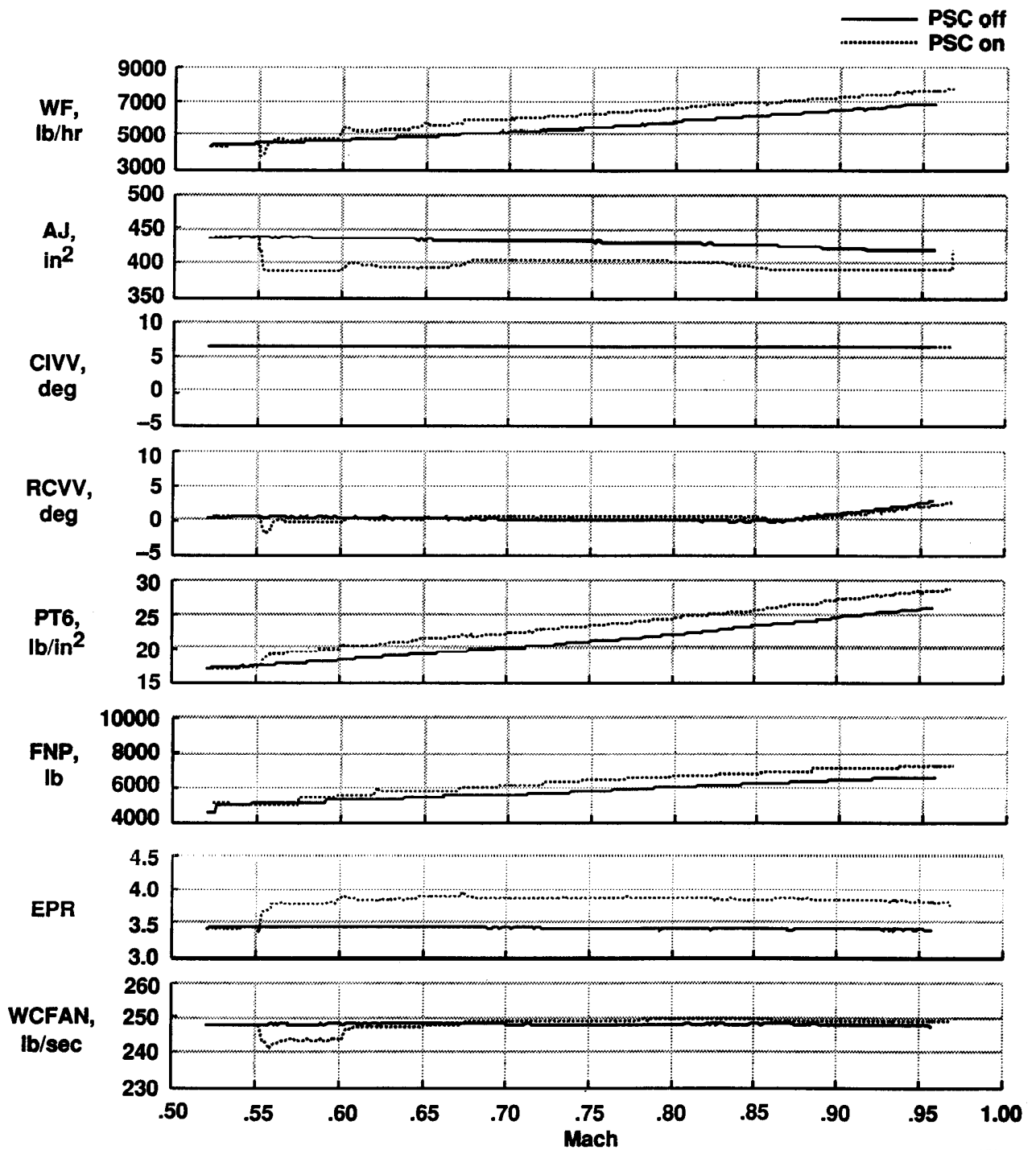
910350

Fig. 7. Engine parameter time histories for minimum *FTIT* mode evaluation; $M = 0.85$, $h = 45,000$ ft, MIL PLA.



910351

Fig. 8. Predicted and measured *FTIT* decreases as a function of flight condition.



910352

Fig. 9. Engine parameter time histories for maximum thrust mode evaluation; $M = 0.50$ to 0.95 , $h = 30,000$ ft, MIL PLA.

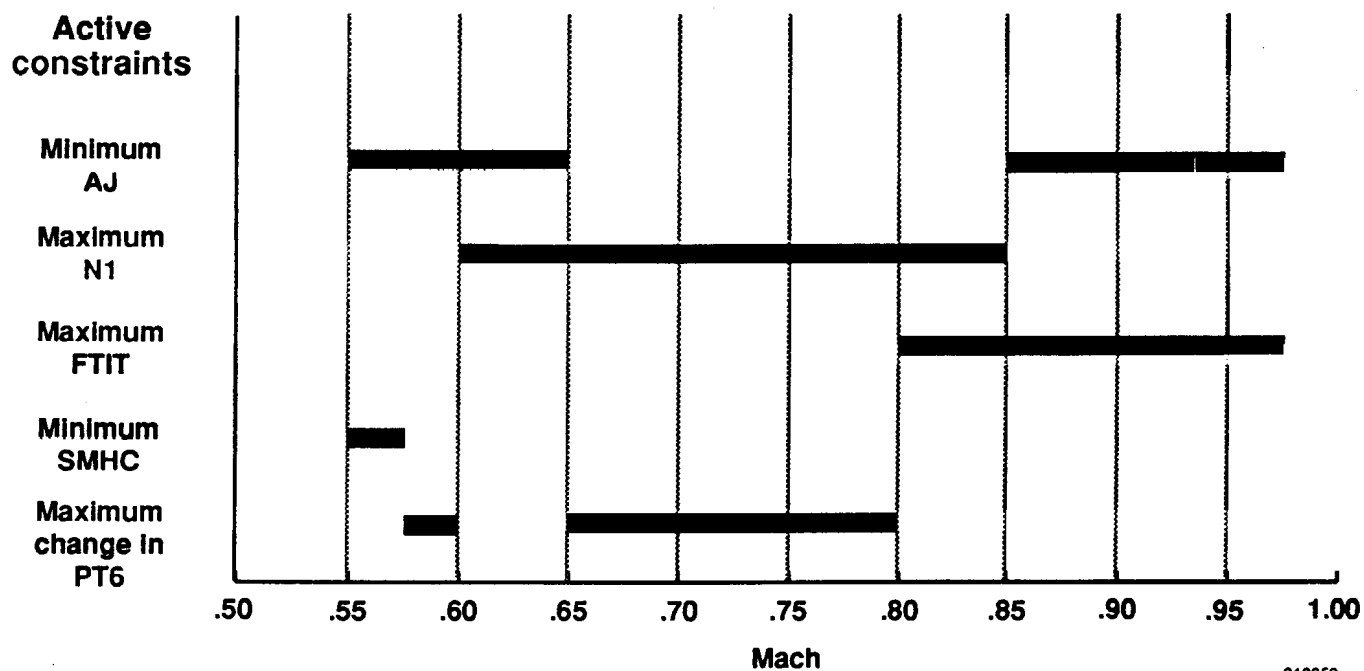


Fig. 10. Linear programming constraints for maximum thrust mode evaluation; $M = 0.50$ to 0.95 , $h = 30,000$ ft, MIL PLA.

REPORT DOCUMENTATION PAGE			Form Approved OMB No. 0704-0188	
Public reporting burden for this collection of information is estimated to average 1 hour per response, including the time for reviewing instructions, searching existing data sources, gathering and maintaining the data needed, and completing and reviewing the collection of information. Send comments regarding this burden estimate or any other aspect of this collection of information, including suggestions for reducing this burden, to Washington Headquarters Services, Directorate for Information Operations and Reports, 1215 Jefferson Davis Highway, Suite 1204, Arlington, VA 22202-4302, and to the Office of Management and Budget, Paperwork Reduction Project (0704-0188), Washington, DC 20503.				
1. AGENCY USE ONLY (Leave blank)	2. REPORT DATE October 1991	3. REPORT TYPE AND DATES COVERED Technical Memorandum		
4. TITLE AND SUBTITLE Preliminary Flight Evaluation of an Engine Performance Optimization Algorithm		5. FUNDING NUMBERS WU-533-02-36		
6. AUTHOR(S) H.H. Lambert, G.B. Gilyard, J.D. Chisholm, and L.J. Kerr				
7. PERFORMING ORGANIZATION NAME(S) AND ADDRESS(ES) NASA Dryden Flight Research Facility P.O. Box 273 Edwards, California 93523-0273		8. PERFORMING ORGANIZATION REPORT NUMBER H-1745		
9. SPONSORING/MONITORING AGENCY NAME(S) AND ADDRESS(ES) National Aeronautics and Space Administration Washington, DC 20546-0001		10. SPONSORING/MONITORING AGENCY REPORT NUMBER NASA TM-4328		
11. SUPPLEMENTARY NOTES Presented at the AIAA/ASME/SAE/ASEE 27th Joint Propulsion Conference, Sacramento, CA, June 24-26, 1991. H.H. Lambert and G.B. Gilyard, NASA Dryden Flight Research Facility; J.D. Chisholm, McDonnell Douglas Corporation, St. Louis, MO; L.J. Kerr, Pratt & Whitney, West Palm Beach, FL.				
12a. DISTRIBUTION/AVAILABILITY STATEMENT Unclassified — Unlimited Subject Category 07			12b. DISTRIBUTION CODE	
13. ABSTRACT (Maximum 200 words) The initial flight test evaluation phase of the performance seeking control (PSC) algorithm has been completed for one engine, subsonic, part power, and military power operation on an F-15 aircraft, using a PW1128 engine. The algorithm is designed to optimize the quasi-steady-state performance of an engine for three primary modes of operation: the minimum fuel, the minimum fan turbine inlet temperature (FTIT), and the maximum thrust modes. The minimum fuel mode is designed to minimize thrust-specific fuel consumption during cruise conditions. The minimum FTIT mode is designed to extend the turbine life by decreasing the FTIT during cruise and accelerating flight conditions. The maximum thrust mode is designed to maximize net propulsive force at military power. Decreases in thrust-specific fuel consumption of approximately 1 percent have been measured in the minimum fuel mode; integrated over the life of the aircraft and fleet size, these fuel savings are significant. Decreases of up to approximately 100 °R in FTIT were measured in the minimum FTIT mode. Temperature reductions of this magnitude are significant and would more than double engine life if FTIT were the only factor. Thrust increases of up to approximately 12 percent were measured in the maximum thrust mode. The system dynamics of the closed-loop algorithm operation appear good. The preliminary flight phase has provided a general validation of the PSC technology which can provide significant benefits to the next generation of fighter and transport aircraft.				
14. SUBJECT TERMS Engine control; Estimation; F-15; F-100 engine; HIDECE; Integrated control; Optimal control: Performance seeking control			15. NUMBER OF PAGES 20	
			16. PRICE CODE A03	
17. SECURITY CLASSIFICATION OF REPORT Unclassified	18. SECURITY CLASSIFICATION OF THIS PAGE Unclassified	19. SECURITY CLASSIFICATION OF ABSTRACT	20. LIMITATION OF ABSTRACT	